CHEMISTRY
A EUROPEAN JOURNAL

DOI: 10.1002/chem.200601259

Continuous Tuning of Cadmium Sulfide and Zinc Sulfide Nanoparticle Size in a Water-in-Supercritical Carbon Dioxide Microemulsion

Carlos A. Fernandez and Chien M. Wai*[a]

Abstract: The size and size dispersion of cadmium sulfide and zinc sulfide semiconductor nanoparticles can be continuously tuned over a wide range of values by adjusting the density of the fluid phase in water-in-supercritical CO_2 microemulsions. The average size of the ZnS nanoparticles decreases linearly from approximately 9.1 to 1.9 nm with increasing fluid density from 0.86 to 0.99 $g\,cm^{-3}$ at a water-to-surfactant ratio (W value) of 10. At a W value of 6, the particle size can be tuned from 7.0 to 1.5 nm in the same density range. In the case of CdS nanocrystals, the size varied from 7.1 to 2.0 nm when the W value was 10 and from 4.0 to 1.3 nm when the W value employed was 6, in the same density range. Monodispersive CdS and ZnS nanoparticles were synthesized by chemical reaction of cadmium or zinc nitrate with sodium sulfide, using two water-in-supercritical CO_2 microemulsions as nanoreactors followed by protection with a fluorinated-thiol stabilizer. The stabilizer is introduced at 6 and 16 minutes after the mixing of the two microemulsions where the intensity of the characteristic absorption peak due to the quantum confinement properties of the CdS and ZnS nanoparticles (280 and 360 nm) reaches a maximum, respectively. The supercritical CO_2 microemulsion method represents a simple approach to use a density-tunable solvent for synthesizing size-controlled semiconductor nanoparticles over a broad range of values.

Keywords: microemulsions · nanoparticles · semiconductors · supercritical carbon dioxide

Introduction

Synthesis of semiconductor quantum dots, such as cadmium sulfide and zinc sulfide nanoparticles, have been largely explored during the last decade due to their size-dependent optical, magnetic and electric properties.[1–3] Luminescence tagging and imaging, medical diagnostics, drug delivery, and nanoelectronics are some of the applications that are being developed with these nanomaterials.[4–8] One of the approaches utilized to synthesize these nanomaterials is the microemulsion-templated method using compressed gases as solvents. Particularly, supercritical carbon dioxide ($scCO_2$) has been used as the bulk solvent in microemulsion systems to prepare semiconductor nanoparticles.[9] Odhe et al.[10] prepared CdS and ZnS nanoparticles in $scCO_2$ using a microemulsion approach. They showed that the size of the quantum dots can be adjusted with the water-to-surfactant molar ratio or W value.

Supercritical fluids (SCFs) have attracted considerable interest as a reaction medium to synthesize nanoparticles,[11–14] because the variations in SCF solvent properties, such as density, diffusivity, viscosity, and dielectric constant, can be easily manipulated by changing the system temperature and pressure.,[15,16] In addition to these advantages, $scCO_2$ provides an attractive substitute for petroleum-based organic solvents for chemical synthesis since it is nontoxic, environmentally-benign, nonflammable, inexpensive, and readily available in large quantities. The unique property of supercritical fluids, including $scCO_2$, is its tunable solvent strength through manipulation of its density (ρ), which can be easily controlled, as mentioned above, by varying temperature and pressure of the fluid phase. This property is attractive for studying nanoparticles' formation using water-in-$scCO_2$ microemulsions as nanoreactors. There are a few reports studying the variation in the size of metallic nanoparticles with the density of the fluid phase. Shah et al.[17] reported the influence of pressure, stabilizer, and precursor concentration in the formation and dispersion of silver nanoparticles obtained by arrested precipitation, where a thiol stabilizer was added together with hydrogen gas (H_2) to a CO_2-soluble metal precursor, silver acetylacetone. In this study, no microemulsion was used for silver nanoparticle synthesis and

[a] C. A. Fernandez, Prof. C. M. Wai
Department of Chemistry, University of Idaho
P.O. Box 442343, Moscow, ID 83844-2343 (USA)
Fax: (+1) 208-885-6173
E-mail: cwai@uidaho.edu

the reaction time was 3 h. At a thiol/precursor ratio of around 2.5 and a temperature of 80 °C, the silver nanoparticles thus synthesized were found to decrease in size with increase in pressure from 4.0 ± 2.1 nm at 207 bar ($\rho = 0.61\ g\,mL^{-1}$) to 1.7 ± 1.1 nm at 259 bar ($\rho = 0.698\ g\,mL^{-1}$). Above that pressure, the average size of the silver nanoparticles remained virtually constant with smaller standard deviations. Synthesis of copper nanoparticles in reverse micelles was performed by Kitchens and Roberts[18] using compressed liquid and supercritical fluid alkanes as the bulk solvent. The size of the nanocrystals was found to increase with pressure. In supercritical propane, the median nanoparticle size (the median instead of the mean diameter was used due to the presence of large particle aggregate outliers) increased from 5.4 to 9.0 nm with increasing pressure from 241 to 345 atm at 21 °C and a W value of 1.5. The size variation did not show a continuous change and in the pressure range 276 to 317 atm the nanoparticle size remained unaltered. The reaction times in these studies were long (2–3 h) and the size dispersions were large and in some cases almost as large as the nanoparticles' median diameter.

We have recently shown, for the first time, that the size of silver nanoparticles can be tuned over a wide range of values by adjusting the density of $scCO_2$.[19] We were able to synthesize silver nanoparticles with sizes ranging from 1.9 to 9.3 nm when $W = 6$ was used and from 5.5 to 13 nm when a higher water-to-surfactant molar ratio ($W = 10$) was employed.

To our knowledge, the variation in size of semiconductor quantum dots with respect to supercritical CO_2 density, have not been explored. In this article, we present a study performed in $scCO_2$ for synthesizing two well-known semiconductor nanocrystals, CdS and ZnS. We demonstrate that the size of CdS and ZnS nanoparticles synthesized in a $scCO_2$ microemulsion, varies linearly with the density of the fluid, in a similar fashion silver nanoparticles have proven. The observation suggests a simple technique for continuous tuning the size of semiconductor nanoparticles synthesized in reverse micelles, using $scCO_2$ as a solvent. This unique technique may have a range of applications for making 2D and 3D arrays of nanoparticles of variable size for new optical materials,[20,21] biosensor-related applications,[22–24] and, when passivated with a wider bandgap material, targeting luminescent probes in biological labeling and diagnostics.[25,26]

Results and Discussion

Figure 1 shows a representative TEM micrograph for the 1*H*,1*H*,2*H*,2*H*-perfluorodecanethiol (F-thiol) stabilized CdS (Figure 1a) and ZnS (Figure 1b) nanoparticles, obtained by evaporation of an acetone solution containing the nanoparticles on a carbon-coated copper grid. The experimental conditions for the nanoparticles shown in Figure 1 were 300 atm, 40 °C for the synthesis of CdS nanoparticles and 350 atm, 40 °C for the synthesis of ZnS nanoparticles. The surfactant concentration (10 mM), W value ($W = 10$), and precursors concentrations ($CdNO_3$ or $ZnNO_3 = 0.3$ M, $Na_2S = 0.6$ M) were equivalent in both situations. Relatively monodispersive nanoparticles were observed with a distinct separation of particles by the stabilizing ligand.

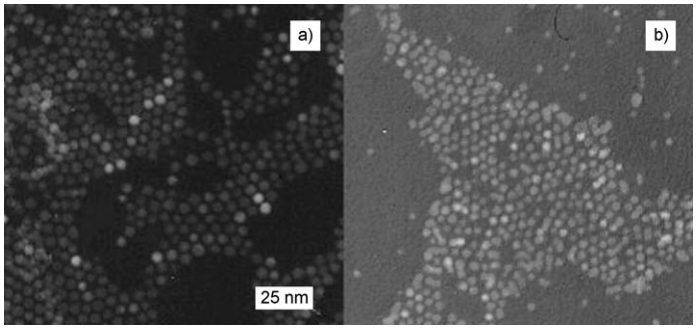

Figure 1. TEM micrographs of the F-thiol-protected a) CdS and b) ZnS nanoparticles with an average diameter of 4.8 and 4.0 nm, respectively. Scale applies to both figures.

Figure 2 shows the variation of the average size of CdS nanoparticles with the fluid pressure when they were synthesized and stabilized according to the procedures described in the Experimental Section at 40 °C. The concentration of the surfactant, sodium bis(2,2,3,3,4,4,5,5-octafluoro-1-pentyl)-2-sulfosuccinate (F-AOT, 10 mM), concentration of precursors and stabilizer, the W value (molar ratio of water/surfactant, $W = 10$) and the temperature (40 °C) of these series of experiments were kept constant and only the pressure of the $scCO_2$ was varied from 220 to 400 atm. The average size of the CdS nanoparticles synthesized by the CO_2 microemulsion method decreases continuously from about 7 ± 1 nm at 220 atm to about 2.9 ± 0.4 nm at 400 atm as shown in Figure 2. The slope of the trend line decreases as the pressure increases. The size distribution of the CdS nanoparticles is larger for the particles formed at low pres-

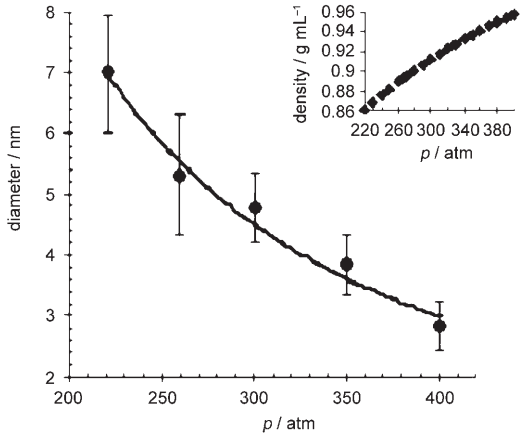

Figure 2. Influence of CO_2 pressure on the average size and size distribution of CdS nanoparticles at 40 °C, $W = 10$, [F-AOT] = 10 mM. Insert: Density versus pressure at a fixed temperature of 40 °C.

sures. The insert on Figure 2 shows the variation of the density of the CO_2 with the pressure at a constant temperature of 40 °C. There is an increment in the density of the solvent as the pressure increases and the slope of this plot decreases as the pressure reaches higher values. The effect of temperature on the size and size distribution of the CdS nanoparticles synthesized by the CO_2 microemulsion method is shown in Figure 3.

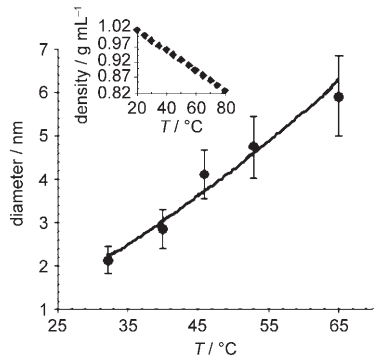

Figure 3. Influence of temperature on the average size and size distribution of CdS nanoparticles at a fixed CO_2 pressure of 400 atm, W = 10, [F-AOT] = 10 mM. Insert: Density versus temperature at 400 atm.

The pressure of this series of experiments was fixed at 400 atm and the temperature varied from 32 to 65 °C. Other parameters including the concentration of the surfactant (in this case, 10 mM), precursors and stabilizer concentrations, and the W value (W = 10) were all kept constant. The average size of the CdS nanoparticles increases continuously with temperature as shown in Figure 3. Again, the size distribution is larger for the larger particles formed at higher temperatures. The density of $scCO_2$ is known to decrease with increasing temperature at a fixed pressure and it is shown in the inserted plot of solvent density versus temperature (at a fixed pressure of 400 atm) in Figure 3. These observations may be an indication that the particle size of the CdS nanoparticles is related to the density of the fluid phase within the temperature and pressure ranges of this study. At this point, it is important to introduce the term Cohesive Energy Density (CED),[27] which is a direct reflection of the degree of van der Waals forces holding molecules together. The CED of the solvent ($scCO_2$) is a function of the fluid density and is higher at increased solvent density (higher p or lower T).[17,28] When the CED of solute and solvent is similar ($scCO_2$ and the fluorinated surfactant tails in the micelles), their intermolecular attractive forces are comparable. Since the solubility of two materials depends on their intermolecular attractive forces, one might expect that materials with similar CED values would be miscible. Under these conditions, the interactions between solvent–surfactant tails are maximized.[28] Therefore, at higher pressures or lower temperatures, the fluorinated surfactant molecules in the micelles may be more solvated and the micelle–micelle interactions become weaker. The result might be a decrease in the amount of materials exchange during collision and smaller particles are obtained.

Another factor to take into account is the influence of the pressure and temperature of the system on the size of the micellar water core. Xu et al.[29] showed that an increment in pressure has an impact in the size of the water droplets. By means of SANS experiments, they found that the size of the water-core decreased by 14% when the pressure was increased from 170 to 380 atm at 27 °C (W = 5 and surfactant concentration 27 mM). The surfactant used in this study was bis[2-(F-hexyl)ethyl] phosphate salts of sodium, and ammonium. In our study, both parameters, micelles' stability through density and water-core size through pressure, might be playing a role in controlling the final nanoparticle size. In order to identify which parameter would lead this size-controlling role, several experiments were carried out with different pressure–temperature combinations, some of them presenting identical fluid densities. For these experiments, where the density was identical but the pressure–temperature conditions were different, the average sizes of the CdS nanocrystals obtained were statistically equivalent. This demonstrates that a variation in the temperature or in the pressure of these water-in-CO_2 microemulsion systems (within the ranges studied here) seems to affect the final nanoparticle's size due *mainly* to a variation in the density of the solvent.

Figure 4a shows a plot of the average CdS nanoparticle size with the $scCO_2$ density using different pressure–temperature combinations, for W = 10. A linear relationship between the average size of the CdS nanoparticles and the density of the fluid phase (in the range 0.86 to 0.99 $g\,cm^{-3}$) is observed. The average size of the semiconductor particles varies from 7 ± 1 nm at 0.86 $g\,cm^{-3}$ to about 2.1 ± 0.3 nm at 0.99 $g\,cm^{-3}$ with a slope of -0.036 nm per ($mg\,mL^{-1}$). The size dispersion varied from 12 to 20% in all the experiments, being in general larger at lower densities. From Figure 4a, it seems possible that a continuous tuning of the CdS nanoparticle size synthesized by the CO_2-microemulsion method could be achieved by varying the density of the fluid in this range. Figure 4b shows the diameter of the nanocrystals as a function of density for W = 6, where the size varied from 4.0 ± 0.5 nm to 1.3 ± 0.2 nm. A linear relationship with a slope of -0.020 nm per ($mg\,mL^{-1}$) similar to the one obtained for W = 10 was observed. This decrease in the size of the nanocrystals with the decrease in the size of the micellar water-core may be due to the fact that there is a change in the hydration of the ions.[30] At very low W values, a small number of ions are free from interacting with the negative heads of the F-AOT surfactant at the surface of the micelle. In this way, the ions are less reactive due to the fact that they have to be pulled away from the micelles' anionic walls. In such cases, the precipitation reaction gives rise to a smaller number of nuclei and the average of the final nanocrystal's size is smaller. Conversely, when the water content is larger (larger W values) there are a larger number of "free" ions and an increment in the reaction yield should be observed. Consequently, the number of

nuclei increases, and the size and production of nanocrystals increases. Our results suggest that the nanoparticle's size follows a linear relationship with the density of the fluid phase and that this trend is independent of the W value or size of the microemulsion. In consequence, by manipulating both parameters, density and W value, the diameter of the nanoparticles could be tuned over even a wider range of values.

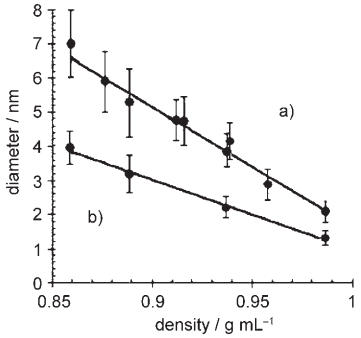

Figure 4. Influence of CO_2 density on the average size and size distribution of CdS nanoparticles, [F-AOT] = 10 mM. a) W = 10; b) W = 6.

The variation of the nanoparticle's diameter with the fluid density was also studied for two different concentrations of surfactant. Figure 5 shows the results, where one of the plots (Figure 5a) was already shown in Figure 4a. In both cases a linear relationship was obtained and the slope of the trend line was -0.030 nm per (mg mL^{-1}) when the concentration of FAOT was 20 mM. An increment in the size of the CdS nanoparticles was observed when a greater surfactant concentration was employed specially at higher densities. The concentration of Cd^{2+} and S^{2-} ions in the water core is constant in all these experiments, but the population of the CO_2 microemulsion increases in the system. The number of collisions between adjacent reverse micelles would increase as a result, and larger nanoparticles should form.[31]

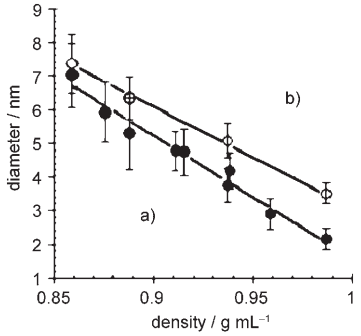

Figure 5. Influence of CO_2 density on the average size and size distribution of CdS nanoparticles, W = 10. a) [F-AOT] = 10 mM; b) [F-AOT] = 20 mM.

Figure 6 shows a representative excitation and emission spectra of the stabilized CdS nanoparticles obtained at two different densities of $scCO_2$. A red shift of 14 nm (from 349 to 363 nm) together with an increment in the Full Width at Half Maximum (FWHM) from 48 to 63 nm, was observed in the excitation spectra when the density of the solvent decreased from 0.92 to 0.87 g mL^{-1} (W = 10 F-AOT concentration 10 mM). This is related to the observed increment in the average size of the CdS particles from 4.7 ± 0.7 to 6.0 ± 0.9 nm, when the synthesis of the materials is carried out at lower fluid densities. The emission spectra are associated to the emission of the surface defects, such as electron-hole pair recombination of surface trap states.,[32,33] Yet again, a red shift in the fluorescence wavelength from 440 to 498 nm was observed when the size of the CdS nanoparticles increased in the range described above.

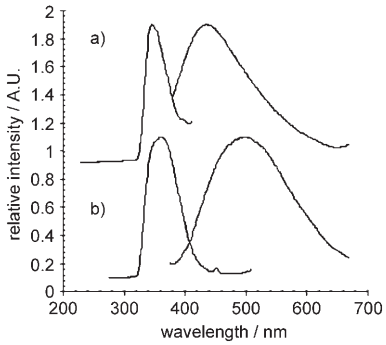

Figure 6. Excitation and emission spectra of CdS nanoparticles obtained at two different fluid densities. a) Spectra of 4.7 nm CdS nanoparticles obtained at a supercritical CO_2 density of 0.92 g mL^{-1}; b) spectra of 6.0 nm CdS nanoparticles obtained at a supercritical CO_2 density of 0.87 g mL^{-1}.

The variation of the size of ZnS nanoparticles with the fluid density was studied by performing experiments in a similar way to that of the CdS nanoparticles. Figure 7 shows a plot of the variation of ZnS nanoparticles with the density of $scCO_2$ for two different W values. For W value of 10 (Figure 7a), the size of the nanoparticles decreased from 9 ± 1 to 1.9 ± 0.3 nm when the density of the solvent increased from 0.86 to 0.99 g mL^{-1}. The slope of the trend line was -0.053 nm per (mg mL^{-1}). When W = 6 was used in the preparation of the microemulsions, the size of the ZnS particles synthesized decreased from 7 ± 1 to 1.5 ± 0.2 nm with a slope of -0.042 nm per (mg mL^{-1}), as shown in Figure 7b. The increment in the average size of the nanoparticles with the size of the micelles (W value) in $scCO_2$ microemulsions is known in the literature,[34,35] and it was described previously for CdS nanoparticles.

When the surfactant concentration was doubled from 10 to 20 mM, the size of the ZnS particles showed a partially different behavior to the one observed for the CdS nanoparticles. In both conditions, the size of the nanoparticles decreased with an increment in the fluid density with a slope of -0.044 nm per (mg mL^{-1}) for the case of F-AOT concentration of 20 mM and similar to the one observed for a surfactant concentration of 10 mM (-0.053 nm per (mg mL^{-1}). Figure 8 shows this behavior, where one of the plots (Fig-

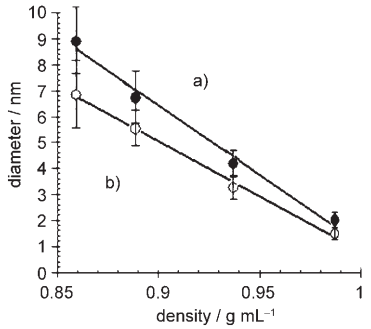

Figure 7. Influence of CO_2 density on the average size and size distribution of ZnS nanoparticles, [F-AOT] = 10 mM. a) W = 10; b) W = 6.

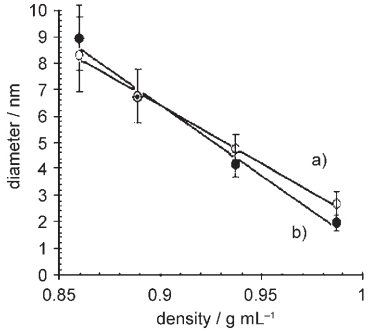

Figure 8. Influence of CO_2 density on the average size and size distribution of ZnS nanoparticles, W = 10. a) [F-AOT] = 20 mM; b) [F-AOT] = 10 mM.

ure 8b) was already shown on Figure 7. It seems that, in contrast to what we observed for CdS nanoparticles, the size of the nanoparticles might be independent of the surfactant concentration, mainly at lower solvent densities. It is important to mention that Natarajan et al.,[36] by means of a modeling approach, found that the size of the nanoparticles was unaffected by changing the surfactant concentration, keeping constant the W value. He predicted that by keeping the W value constant, while increasing or decreasing proportionally the water and surfactant concentration, the aqueous core volume would remain constant. Therefore, according to his study, the size and size distribution of the nanoparticles should be unaffected. This group cited the experimental case of silver nanoparticles synthesized in water-in-oil microemulsions, where an increment in the surfactant concentration (keeping constant the rest of the parameters, including the W value) produced an increase in the number of particles formed without any changes in the average size. Consequently, the influence of the surfactant concentration on the final nanoparticle size seems to depend on the nanoparticle nature and solvent, and may raise a question whether the collision frequency plays a role in the final particle size at all.

We performed some experiments using different pressure–temperature combinations with similar density values. For these experiments, the average sizes of the ZnS nanocrystals obtained were statistically equivalent, demonstrating as in the case of CdS nanoparticles, that a variation in the temperature or in the pressure of these water-in-CO_2 microemulsion systems (within the ranges studied here) may affect the final nanoparticle's size due mainly to a variation in the density of the solvent. On Figure 9, the excitation and

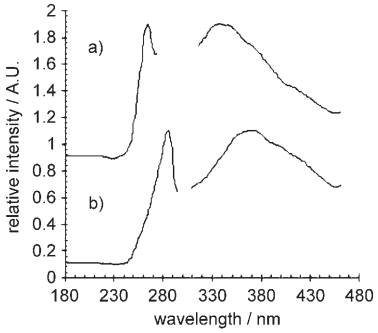

Figure 9. Excitation and emission spectra of ZnS nanoparticles obtained at two different fluid densities. a) Spectra of 2.0 nm ZnS nanoparticles obtained at a supercritical CO_2 density of 0.99 g mL^{-1}; b) spectra of 6.7 nm ZnS nanoparticles obtained at a supercritical CO_2 density of 0.89 g mL^{-1}.

emission spectra of the stabilized ZnS nanoparticles obtained at two different densities of carbon dioxide are shown. A red shift of 23 nm (from 263 to 286 nm) and an increment in the FWHM from 22 to 30 nm, are observed in the excitation spectra when the density of the solvent decreased from 0.99 to 0.89 g mL^{-1}. These results are in agreement with an increment in the average size of the ZnS particles from 2.0 ± 0.3 to 6.7 ± 0.9 nm, when the synthesis of the materials is carried out at lower fluid densities. Similarly to what we observed for CdS nanoparticles, the emission spectra of ZnS nanoparticles appear to be due to the surface defects,[37,38] with a red shift in the fluorescence wavelength from 340 to 373 nm when the size of the ZnS nanoparticles increased. Fluorinated-thiol seems not to be effective for passivation of the surface defects on CdS and ZnS nanoparticles.

The reaction time is another factor that may influence the size of the CdS and ZnS nanoparticles synthesized by the CO_2-microemulsion method. In the case of the synthesis of CdS nanoparticles we decided to discontinue the reaction after six minutes to avoid further aggregation as indicated by our spectroscopic observation (through a red shift and a decrease in the absorption peak) when the reaction time was extended (see Experimental Section for details). By increasing the reaction time to 90 minutes, the average size of the CdS nanoparticles (obtained by analysis of the TEM data) increased from 7.0 ± 0.9 to 12 ± 2 nm when $scCO_2$ at 220 atm and 40 °C was employed ([FAOT] = 10 mM, W = 10). Tuning of CdS nanoparticles by density variation appears to work well at short reaction times where the exchange-channel mechanism and the micellar-templating effect dominate. For very long reaction times, as the nanoparticles grow larger, the surfactant might act as a dispersant ligand[18] and

sterically stabilizes the nanoparticles without involving the microemulsion. Conversely, in the case of ZnS nanoparticles, the reaction time seems not to affect the final particle size. When the reaction time was extended from 16 to 90 minutes, the size of the nanoparticles remained statistically unchanged. This result is in agreement with the spectroscopic study performed during the synthesis of ZnS nanoparticles, showing an increment in the absorption maximum (at 280 nm) in the first 16 minutes and remaining constant afterwards for at least 120 minutes. The reason for this behaviour is uncertain but might be related to a different mechanism of formation of the nanoparticles and/or to a better stabilization of the ZnS nanoparticles by the micelle system (once they reach the final size) against further aggregation.

Conclusion

In summary, we have shown that the size of CdS and ZnS nanoparticles synthesized by the $scCO_2$ microemulsion-templating method can be continuously tuned by density variation of the fluid phase, in a similar fashion as we demonstrated previously for Ag nanoparticles.[19] This approach gave consistent results in both nanomaterials for two different W values and for two different concentrations of surfactant tested. For the case of ZnS nanoparticles, the variation in the size of the nanoparticles with the density of the solvent (which follows a linear relationship) may not depend on the stage of the synthetic process at which the nanoparticles are stabilized. On the other hand, the time at which the stabilization of CdS nanoparticles takes place seems to be crucial to avoid further aggregation. Other parameters like the nature of the nanoparticles and the solvent may affect as well.

This study, together with the one reported for silver nanoparticles,[19] have shown, that water-in-supercritical CO_2 microemulsions seem to be effective systems for the tunable-size synthesis of a diversity of nanomaterials by varying the density of the fluid.

Experimental Section

The surfactant used in this study, sodium bis(2,2,3,3,4,4,5,5-octafluoro-1-pentyl)-2-sulfosuccinate (F-AOT), was prepared in our lab following the procedure by Liu and Erkey[39] with some modification. Cadmium nitrate ($Cd(NO_3)_2$), was obtained from Aldrich with purity 99.999%, zinc nitrate ($Zn(NO_3)_2$) was obtained form Fisher Scientific with a purity of 99.1%, while sodium sulfide (Na_2S >99.8%) was obtained from Aldrich. The stabilizer or protecting agent, 1*H*,1*H*,2*H*,2*H*-perfluorodecanethiol (F-thiol) 97% was purchased from Aldrich.

The liquid CO_2 was metered with an ISCO syringe pump (model 260 D) and pump controller (series D) and introduced to the high-pressure reactors via stainless steel tubing ($^1/_{16}$ inch o.d., 0.03 inch i.d.). The high-pressure vessels were heated with a thermal block and the temperature was kept constant at ± 0.1 °C and controlled with a J-type sensor and an Omega digital controller. Three homemade high-pressure vessels were utilized. One vessel (18.5 mL volume) was equipped with a fiber-optic system (3 mm path length) and connected to a CCD array UV-VIS spectrometer (Spectral Instruments model SI-440, Tucson, AZ).[40] The spectrometer is capable of recording a full spectrum from 240 to 900 nm in 2 s. It can also measure the change in absorbance with time at a fixed specific wavelength. The second vessel was a 17 mL high-pressure view cell with sapphire windows. The last one was a 17.5 mL vessel with a movable piston. The high-pressure vessels were connected to each other via $^1/_{16}$ in stainless steel tubing. Each system was isolated from the others by HIP high-pressure valves.

The cloud points for the microemulsion containing the Cd^{2+} ions, Zn^{2+} ions and the CdS and ZnS nanoparticles were studied using a view-cell connected to a piston (both immersed in a thermal bath) and by visual observation of the phase behavior. At 40 °C, a W (water to surfactant ratio) value of 10, and a surfactant concentration of 10 mM, the cloud point of a Cd^{2+} ion (Aqueous concentration 0.3 M) microemulsion was found to be 145 ± 2 atm. In the case of Zn^{2+} ion (Aqueous concentration 0.3 M) the cloud point was 130 ± 2 atm under identical conditions. Above these pressures at 40 °C, the microemulsion is stable and is optically transparent. The cloud point boundary is approximately linear in a pressure versus temperature plot with a slope of 3.63 atm °C^{-1} for the case of Cd^{2+} microemulsions, and with a slope of 2.50 atm °C^{-1} for the case of Zn^{2+} microemulsions. Our experiments were performed above the cloud point pressure to the limit of our high pressure system which is about 450 atm. The variation in density of $scCO_2$ at different temperature and pressure is known.[41]

The semiconductor nanoparticles were synthesized by mixing two water-in-supercritical CO_2 ($scCO_2$) microemulsions, one containing a cadmium nitrate solution or zinc nitrate solution (0.3 M) and the other containing an aqueous solution of sodium sulfide (0.6 M). The microemulsion containing the sulfur ion was pushed into the metal ions' microemulsion using the piston cell. Formation of the CdS and ZnS nanoparticles after the mixing was monitored spectroscopically, using the optical fiber cell, by taking the absorption spectra in situ every two seconds. A blank measurement was taken before the reaction to provide a spectroscopic baseline, using a water-in-$scCO_2$ microemulsion containing deionized water. The characteristic absorption peak due to the quantum confinement properties of CdS nanoparticles ($\lambda \approx 330$ nm) was found to increase to a maximum at about 6 min after the mixing, and started to decrease gradually in intensity and reached a plateau in about 125 minutes. A red shift of 33 nm (330 to 363 nm) of the absorption peak wavelength, when going from 6 to 90 min of reaction time was noticed. This, together with the decrease in the peak intensity, should indicate that the concentration of the nanoparticles reaches a maximum in the first 6 min and it is followed by a decrease in their concentration, probably attributable to aggregation.[42] In the case of ZnS nanoparticle synthesis, the characteristic absorption peak appeared at 280 nm and it was found to increase and reach a plateau after 16 min. At that point of the reaction the peak intensity was constant (remaining in that way for more than 120 min). It seems that, unlike the CdS nanoparticles, ZnS nanoparticles do not experience further aggregation after they reach the final size.

In the case of CdS nanoparticle synthesis, the F-thiol stabilizer (1*H*,1*H*,2*H*,2*H*-perfluorodecanethiol) was introduced to the system, via a six-port injector valve, at exactly 6 min after the mixing; while in the case of ZnS nanoparticle synthesis, the stabilizer was added after the first 16 min. The F-thiol-stabilized CdS or ZnS nanoparticles were collected in an acetone solution after depressurizing the system for TEM measurements. The protected semiconductor nanoparticles are stable in acetone or ethanol for several days and the unprotected CdS and ZnS nanoparticles in either solvent would precipitate after approximately 15 min. TEM images were obtained with a JEOL 1200 EX II transmission electron microscope at an accelerating voltage of 120 kV. EDS analysis was carried out with a LEO Supra 35 VP Field Emission Scanning Electron Microscope (FESEM). EDS analysis of the stabilized nanoparticles showed only cadmium or zinc, carbon, oxygen, fluorine, sulfur and sodium in the samples. The last one may be coming originally from the sodium sulfide precursor. The average size of the nanoparticles was obtained from the TEM micrographs by counting at least 300 particles using interactive imaging software (Matrox Inspector) from Matrox Electronic Systems

(Dorval, Quebec, Canada). An important feature of this software is that it can measure a large number of particles without bias or human error.

Acknowledgements

This work was supported by a grant from DOD-AFOSR (F49620-03-1-0361) and by the Idaho DOE-EPSCoR program (DE-FG02-04ER46142).

[1] A. P. Alivisatos, *Science* **1996**, *271*, 933–937.
[2] C. Tojo, M. C. Blanco, M. A. Lopez-Quintela, *Langmuir* **1997**, *13*, 4527–4534.
[3] R. Rosetti, R. Hull, J. M. Gibson, L. E. Brus, *Chem. Phys.* **1985**, *82*, 552–559.
[4] a) C. M. Niemeyer, *Angew. Chem.* **2001**, *113*, 4254–4287; b) C. M. Niemeyer, *Angew. Chem. Int. Ed.* **2001**, *40*, 4128–4158.
[5] C. A. Mirkin, *Inorg. Chem.* **2000**, *39*, 2258–2272.
[6] S. R. Whaley, D. S. English, E. L. Hu, P. F. Barbara, A. M. Belcher, *Nature* **2000**, *405*, 665–668.
[7] D. Ishii, K. Kinbara, Y. Ishida, N. Ishii, M. Okochi, M. Yohda, T. Aida, *Nature* **2003**, *423*, 628–632.
[8] M. J. Meziani, Y.-P Sun, *J. Am. Chem. Soc.* **2003**, *125*, 8015–8018.
[9] J. D. Holmes, P. A. Bhargava, B. A. Korgel, K. P. Johnston, *Langmuir* **1999**, *15*, 6613–6615.
[10] H. Ohde, M. Ohde, F. Bailey, H. Kim, C. M. Wai, *Nano Lett.* **2002**, *2*, 721–724.
[11] P. S. Shah, J. D. Holmes, R. C. Doty, K. P. Johnston, B. A. Korgel, *J. Am. Chem. Soc.* **2000**, *122*, 4245–4246.
[12] P. S. Shah, J. D. Holmes, K. P. Johnston, B. A. Korgel, *J. Phys. Chem. B* **2002**, *106*, 2545–2551.
[13] P. S. Shah, S. Husain, K. P. Johnston, B. A. Korgel, *J. Phys. Chem. B* **2002**, *106*, 12178–12185.
[14] J. P. Cason, K. Khambaswadkar, C. B. Roberts, *Ind. Eng. Chem. Res.* **2000**, *39*, 4749–4755.
[15] M. A. McHugh, V. J. Krukonis, *J. Supercritical Fluid Extraction*, 2nd ed., Butterworth Heinemann, Boston, MA, **1994**.
[16] M. Poliakoff, P. King, *Nature* **2001**, *412*, 125.
[17] P. S. Shah, H. Shabbir, K. P. Johnston, B. A. Korgel, *J. Phys. Chem. B* **2002**, *106*, 12178–12185.
[18] C. L. Kitchens, C. B. Roberts, *Ind. Eng. Chem. Res.* **2004**, *43*, 6070–6081.
[19] C. A. Fernandez, C. M. Wai, *Small* **2006**, *2*, 1266–1269.
[20] J.-P. Boilot, J. Biteau, A. Brun, F. Chaput, T. D. De Morais, B. Darracq, T. Gacoin, K. Lahlil, J.-M. Lehn, Y. Levy, L. Malier, G.-M. Tsivgoulis, *Mater. Res. Soc. Symp. Proc.* **1998**, *519*, 227.
[21] J. Y. Kim, H. Hiramatsu, F. E. Osterloh, *J. Am. Chem. Soc.* **2005**, *127*, 15556–15561.
[22] V. Pardo-Yissar, E. Katz, J. Wasserman, I. Willner, *J. Am. Chem. Soc.* **2003**, *125*, 622–623.
[23] M. L. Curri, A. Agostiano, G. Leo, A. Mallardi, P. Cosma, M. D. Monica, *Mater. Sci. Eng. C* **2002**, *22*, 449–452.
[24] E. Katz, A. N. Shipway, I. Willner, *Nanoscale Materials* (Eds.: L. M. Liz-Marzan, P. Kamat), Kluwer, **2003**, pp. 5–78.
[25] S. Santra, P. H. Holloway, R. A. Mericle, H. Yang, *US Patent Application*, serial number 60/567330, **2004**.
[26] T.-C. Liu, Z.-L. Huang, H.-Q. Wang, Y.-D. Zhao, Q.-M. Luo, *Proc. SPIE-Int. Soc. Opt. Eng.* **2006**, 6026.
[27] J. Burke, *AIC Book and Paper Group Annual, Vol. 3* (Ed.: C. Jensen), American Institute for Conservation of Historic and Artistic Works Publisher, Washington, DC, **1984**, pp. 13.
[28] M. L. O'Neill, Q. Cao, M. Fang, K. P. Johnston, S. P. Wilkinson, C. D. Smith, J. L. Kerschner, S. H. Jureller, *Ind. Eng. Chem. Res.* **1998**, *37*, 3067–3079.
[29] B. Xu, G. W. Lynn, J. Guo, Y. B. Melnichenko, G. G. Wignall, J. B. McClain, J. M. DeSimone, C. S. Johnson, Jr., *J. Phys. Chem. B* **2005**, *109*, 10261–10269.
[30] L. Motte, I. Lisiecki, M. P. Pileni, in *Hydrogen Bond Networks* (Eds.: J. C. Dore, M. C. Bellissent-Funel), NATO publisher, **1994**, pp. 447.
[31] L. Magagnin, V. Bertani, P. L. Cavallotti, R. Maboudian, C. Carraro, *Microelectron. Eng.* **2002**, *64*, 479–478.
[32] W. Xu, Y. Liao, D. L. Akins, *J. Phys. Chem. B* **2002**, *106*, 11127–11131.
[33] B. Liu, G. Q. Xu, L. M. Gan, C. H. Chew, W. S. Li, Z. X. Shen, *J. Appl. Phys.* **2001**, *89*, 1059.
[34] H. Ohde, M. Ohde, K. H. Bailey, C. M. Wai, *Nano Lett.* **2002**, *2*, 721–724.
[35] S. S. Honga, M. S. Leea, H. S. Hwangb, K. T. Lim, S. S. Parka, C. S. Jua, G. D. Leea, *Solar Energy Materials Sol. Cells* **2003**, *80*, 273–282.
[36] U. Natarajan, K. Handique, A. Mehra, J. R. Bellare, K. C. Khilar, *Langmuir* **1996**, *12*, 2670–2678.
[37] H. C. Warada, S. C. Ghosha, B. Hemtanona, C. Thanachayanontb, J. Duttaa, *Sci. Technol. Adv. Mater.* **2005**, *6*, 296–301.
[38] E. A. Turner, Y. Huang, J. F. Corrigan, *Eur. J. Inorg. Chem.* **2005**, 4465–4478.
[39] Z.-T. Liu, C. Erkey, *Langmuir* **2001**, *17*, 274–277.
[40] H. Ohde, F. Hunt, C. M. Wai, *Chem. Mater.* **2001**, *13*, 4130–4135.
[41] National Institute of Standards and Technology, "*Thermophysical Properties of Fluid Systems*", can be found under: http://webbook.nist.gov/chemistry/flui
[42] J. Liu, P. Raveendran, Z. Shervani, Y. Ikushima, Y. Hakuta, *Chem. Eur. J.* **2005**, *11*, 1854–1860.

Received: September 1, 2006
Revised: January 13, 2007
Published online: April 19, 2007

